

# Ferroelectric Transition Vanishes in $(\text{NH}_4)_2\text{SO}_4$ Precipitated in Small-Sized Aqueous Droplets

Anatoli Bogdan,<sup>\*,†,‡,§</sup> Mario J. Molina,<sup>⊥</sup> Heikki Tenhu,<sup>‡</sup> Tuukka Petäjä,<sup>§</sup> and Thomas Loerting<sup>†</sup>

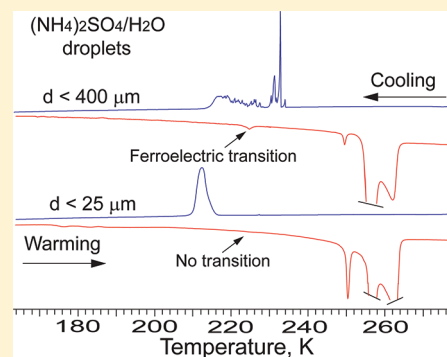
<sup>†</sup>Institute of Physical Chemistry, University of Innsbruck, Innrain 52a, A-6020 Innsbruck, Austria

<sup>‡</sup>Laboratory of Polymer Chemistry, Department of Chemistry, P.O. Box 55, University of Helsinki, FI-00014 Helsinki, Finland

<sup>§</sup>Department of Physics, P.O. Box 48, University of Helsinki, FI-00014 Helsinki, Finland

<sup>⊥</sup>Department of Chemistry and Biochemistry, University of California, San Diego, La Jolla, California 92093-0356, United States

**ABSTRACT:** The ferroelectric transition of  $(\text{NH}_4)_2\text{SO}_4$  precipitated during the freezing of aqueous ammonium sulfate droplets is investigated by means of differential scanning calorimetry (DSC). Below 223 K ammonium sulfate precipitates into ferroelectric crystals from (single) millimeter-sized and (emulsified) large micrometer-sized droplets. Upon subsequent warming, the ferro- to paraelectric (F  $\rightarrow$  P) transition is observed at  $\sim 223$  K. In the case of (emulsified) small micrometer-sized droplets,  $(\text{NH}_4)_2\text{SO}_4$  precipitates into the paraelectric phase, and the F  $\rightarrow$  P transition is absent. Since the mass sensitivity of the DSC instrument is demonstrated to be high enough to resolve the possible F  $\rightarrow$  P transition of  $(\text{NH}_4)_2\text{SO}_4$  precipitated in small-sized droplets, this suggests that  $(\text{NH}_4)_2\text{SO}_4$  crystals precipitated from small micrometer-sized droplets are smaller than the critical size, below which ferroelectric ammonium sulfate does not exist. We do not know the exact critical size, but from independent measurements on  $(\text{NH}_4)_2\text{SO}_4$  aerosol particles, we estimate it to be less than 100 nm. These results can be useful for nanoscience, the theory of  $(\text{NH}_4)_2\text{SO}_4$  ferroelectricity, and the atmosphere where submicrometer-sized  $(\text{NH}_4)_2\text{SO}_4$  aerosol particles are abundant cloud nuclei.



## INTRODUCTION

Studies of ferroelectrics have revealed finite size effects such as the diffuse (smeared) ferroelectric transition and lowering of the Curie temperature,  $T_c$ , with decreasing dimensions and the existence of a critical size below which ferroelectricity collapses.<sup>1–9</sup> The critical size of technologically important ferroelectrics of  $\text{SrBi}_2\text{Ta}_2\text{O}_9$  and  $\text{PbTiO}_3$  was estimated to be  $\sim 2.6$  nm<sup>1</sup> and 8.2 nm,<sup>2</sup> respectively. For films, the critical thickness of 1.2 nm for  $\text{PbTiO}_3$  was predicted by *ab initio* calculations<sup>7</sup> and confirmed by synchrotron X-ray scattering<sup>3</sup> and by X-ray photoelectron diffraction.<sup>7</sup> The critical thickness of 2.4 nm for  $\text{BaTiO}_3$  film was calculated from first principles,<sup>8</sup> whereas subsequent measurements with piezoresponse force microscopy showed that robust ferroelectricity exists down to 1 nm in  $\text{BaTiO}_3$  films.<sup>9</sup>

Ammonium sulfate,  $(\text{NH}_4)_2\text{SO}_4$ , is also ferroelectric with  $T_c \approx 223$  K.<sup>10–19</sup> However, the finite size effects in  $(\text{NH}_4)_2\text{SO}_4$  have not been studied, perhaps because  $(\text{NH}_4)_2\text{SO}_4$  is of no technological importance. Besides scientific curiosity, the study of the finite size effects in  $(\text{NH}_4)_2\text{SO}_4$  can cast additional light on the important problems of nanoscience such as the size effects on the structure and properties of small particles. It can be also useful for the theory of ferroelectric transition of  $(\text{NH}_4)_2\text{SO}_4$  and atmospheric physics and chemistry. Despite many attempts at investigating with many experimental techniques,<sup>10–19</sup> the mechanism of the ferroelectric transition of  $(\text{NH}_4)_2\text{SO}_4$  remains not fully understood. A number of

mechanisms and theories of ferroelectric transition have been proposed which include sudden distortions in the  $\text{SO}_4^{2-}$  ions, a so-called point charge model,<sup>16</sup> an order–disorder mechanism,<sup>17</sup> the soft mode theory<sup>18</sup> (however, the soft  $B_{1u}$  mode, which is the main hypothesis of this theory, was not detected in the IR spectrum),<sup>19</sup> etc. According to the most recent theory,<sup>10</sup> the ferroelectric transition is initiated by the reorientation of the whole group of  $\text{NH}_4^+(\text{I})-(\text{SO}_4^{2-})-\text{NH}_4^+(\text{II})$ , where  $\text{NH}_4^+(\text{I})$  and  $\text{NH}_4^+(\text{II})$  are the two nonequivalent ammonium ions of the unit cell. Since ferroelectrics possess an ordered domain structure,<sup>20</sup> one would expect that decreasing size of  $(\text{NH}_4)_2\text{SO}_4$ , and concomitant increasing surface effects may perturb the reorientation of such relatively large  $\text{NH}_4^+(\text{I})-(\text{SO}_4^{2-})-\text{NH}_4^+(\text{II})$  molecular groups and consequently perturb domain formation. In the atmosphere, minuscule  $(\text{NH}_4)_2\text{SO}_4$  particles are believed to serve as ice nuclei and therefore impact on cirrus formation.<sup>21</sup> They may also supply surfaces for heterogeneous chemical reactions. Since  $\text{H}_2\text{O}$  possess a dipole moment, the presence or absence of electric polarization at the  $(\text{NH}_4)_2\text{SO}_4$  surface may affect water uptake and consequently ice nucleation from the vapor phase (deposition mode)<sup>22</sup> and surface chemistry, which was reported to depend on surface polarization.<sup>23–26</sup> Recalling electrofreezing,<sup>27</sup> the presence of

Received: March 13, 2012

Revised: March 31, 2012

Published: April 6, 2012

polarization may also affect the freezing of atmospheric droplets which come into contact with  $(\text{NH}_4)_2\text{SO}_4$  particles (so-called contact freezing mechanism).<sup>22</sup> In this paper, we show that  $(\text{NH}_4)_2\text{SO}_4$  crystals, which precipitate during the freezing of small micrometer-sized droplets below  $T_c \approx 223$  K, do not form the ferroelectric phase, whereas the  $(\text{NH}_4)_2\text{SO}_4$  crystals precipitated in larger micrometer-sized droplets produce the ferroelectric phase. This suggests that similar to other ferroelectrics a critical size of  $(\text{NH}_4)_2\text{SO}_4$  should exist below which the ferroelectric phase cannot be formed.

## EXPERIMENTAL METHOD

For the study of the finite size effects in  $(\text{NH}_4)_2\text{SO}_4$ , we employed micrometer-scaled  $(\text{NH}_4)_2\text{SO}_4/\text{H}_2\text{O}$  droplets in the size range of  $\sim 1$ – $400$   $\mu\text{m}$  which were subjected to the cooling/warming cycle between 278 and 133 K. Micrometer-scaled  $(\text{NH}_4)_2\text{SO}_4/\text{H}_2\text{O}$  droplets were produced by emulsifying 15–38 wt %  $(\text{NH}_4)_2\text{SO}_4$  solutions as described elsewhere.<sup>28–30</sup> The solutions were prepared by mixing 99.99%  $(\text{NH}_4)_2\text{SO}_4$  crystals (Sigma-Aldrich) with ultrapure water. A mixture of 80 wt % halocarbon oil series 0.8 + 20 wt % lanolin was used as oil/surfactant matrix. The ferroelectric transition in  $(\text{NH}_4)_2\text{SO}_4$  was analyzed from thermograms obtained by a Mettler Toledo DSC 822 calorimeter. The calorimetric measurements were performed at a programmed scanning rate of 3 K/min. The details of calorimeter calibration and measurements are described elsewhere.<sup>28</sup> Emulsion samples of the mass of  $\sim 25 \pm 3$  and  $\sim 60 \pm 3$  mg were placed in Al and Au crucibles of the volume of 40  $\mu\text{L}$ . Optical microscope measurements show that the size (diameter) of smallest droplets is less than  $\sim 1$   $\mu\text{m}$  in all emulsions. By varying emulsification time and shaking (stirring) rate, we are able to produce emulsions with different diameter of the largest droplets. For example, emulsions with droplet diameter distributions of  $\sim 1$ – $20$   $\mu\text{m}$ ,  $\sim 1$ – $50$   $\mu\text{m}$ , etc., were obtained by progressively reducing shaking time and rate. The largest droplets were  $\sim 400$   $\mu\text{m}$  in diameter. The “mass sensitivity” of the Mettler Toledo DSC 822 calorimeter has been assessed by measuring the ferroelectric transition in finely powdered  $(\text{NH}_4)_2\text{SO}_4$  crystals,  $\sim 1 \pm 0.2$   $\mu\text{m}$ , which were produced by milling of 99.99%  $(\text{NH}_4)_2\text{SO}_4$  crystals using a mortar and pestle.

## RESULTS AND DISCUSSION

Recently, we reported that the ferroelectric transition at  $T_c \approx 223$  K occurs in  $(\text{NH}_4)_2\text{SO}_4$  precipitated during the second freezing event of millimeter-scaled  $(\text{NH}_4)_2\text{SO}_4/\text{H}_2\text{O}$  droplets.<sup>31,32</sup> Freezing behavior of such droplets is briefly summarized because it will be needed for a better understanding of the discussion below. Figure 1 displays cooling/warming DSC thermograms obtained from a 25 wt %  $(\text{NH}_4)_2\text{SO}_4$  droplet. The two freezing events are due to the freezing out of pure ice (warm truncated exothermic peak) and the freezing of a residual freeze-concentrated solution.<sup>31</sup> The residual solution is formed by the expulsion of  $\text{NH}_4^+$  and  $\text{SO}_4^{2-}$  ions from the ice lattice during the nucleation and growth of ice. Since the residual solution freezes at temperature  $T < 223$  K,  $(\text{NH}_4)_2\text{SO}_4$  precipitates directly into the ferroelectric phase and experiences the  $F \rightarrow P$  transition at  $\sim 223$  K upon warming. The second freezing event can occur also at  $T > 223$  K.<sup>31</sup> In this case the para- to ferroelectric,  $P \rightarrow F$ , transition is observed upon further cooling and the  $F \rightarrow P$  transition upon subsequent warming. The  $F \rightarrow P$  or both the  $P \rightarrow F$  and  $F$

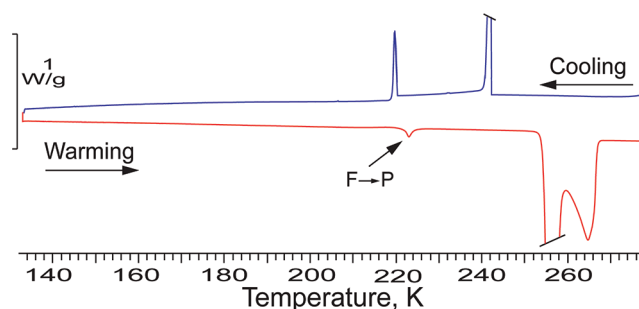


**Figure 1.** Cooling (blue line) and warming thermograms obtained from a millimeter-scaled 25 wt %  $(\text{NH}_4)_2\text{SO}_4$  droplet (5.64 mg) placed in a gold (Au) crucible. The ferro- to paraelectric transition at  $\sim 223$  K is marked as  $F \rightarrow P$ . The scale bar denotes the heat flow through the droplet. The skewed lines truncate the ice freezing and ice/ $(\text{NH}_4)_2\text{SO}_4$  eutectic melting peaks to fit the figure.

$\rightarrow P$  transitions are always observed during the cooling/warming of subeutectic ( $< 40$  wt %  $(\text{NH}_4)_2\text{SO}_4$ ) millimeter-scaled  $(\text{NH}_4)_2\text{SO}_4/\text{H}_2\text{O}$  droplets. In the warming thermogram, the two large endothermic processes are the eutectic melting of ice/ $(\text{NH}_4)_2\text{SO}_4$  (truncated peak) and the melting of pure ice (Figure 1).

Figure 2 presents cooling/warming thermograms obtained from emulsified micrometer-scaled 35 and 38 wt %  $(\text{NH}_4)_2\text{SO}_4$  droplets and only warming thermograms (for the clarity of the figure) obtained from 15–33 wt %  $(\text{NH}_4)_2\text{SO}_4$  droplets. The freezing temperatures of 15–33 wt %  $(\text{NH}_4)_2\text{SO}_4$  droplets are collected in Figure 10 of ref 32. In contrast to millimeter-scaled droplets, the  $F \rightarrow P$  transition is seen only in the warming thermogram of 38 wt %  $(\text{NH}_4)_2\text{SO}_4$  droplets. It is absent in other thermograms despite the fact that  $(\text{NH}_4)_2\text{SO}_4$  crystals precipitate in the samples of all concentrations. The presence of the ice/ $(\text{NH}_4)_2\text{SO}_4$  eutectic melting, which begins at  $\sim 254.5$  K, is a proof that  $(\text{NH}_4)_2\text{SO}_4$  crystals exist indeed.<sup>31</sup> Other peculiarities of the low-temperature behavior of micrometer-scaled droplets, such as the appearance of a single freezing event, the glass transition at  $T_g \approx 172$  K, and the two freezing–crystallization events upon warming are discussed elsewhere.<sup>28</sup>

The area under the transition peaks is proportional to the enthalpy released/absorbed during the first-order phase transition and, consequently, to the amount of material undergoing the phase transition.<sup>34</sup> Since the  $P \rightarrow F$  and  $F \rightarrow P$  transitions are accompanied by the emission and absorption of transition enthalpy, they are considered to be first-order phase transitions.<sup>11,17</sup> One may assume that the absence of the  $F \rightarrow P$  transition in the 15–35 wt %  $(\text{NH}_4)_2\text{SO}_4$  thermograms in Figure 2 could be a result of one of the following options: (i) a small total amount of  $(\text{NH}_4)_2\text{SO}_4$  dispersed in numerous droplets ( $\sim 10^6$ ) of emulsion samples,<sup>30</sup> (ii) the used calorimeter is not sensitive enough to detect the enthalpy released during the  $F \rightarrow P$  transition, (iii) the oil/lanolin matrix, in which  $(\text{NH}_4)_2\text{SO}_4/\text{H}_2\text{O}$  are embedded, brings about disappearance of the  $F \rightarrow P$  transition, or (iv) ammonium sulfate has precipitated into the paraelectric phase even below 223 K; i.e., similar to other ferroelectric, a critical size of  $(\text{NH}_4)_2\text{SO}_4$  may exist below which the ferroelectric phase cannot be formed.

To test the first option, we measured 25–35 wt %  $(\text{NH}_4)_2\text{SO}_4$  emulsion samples of increased mass,  $\sim 60 \pm 3$  mg. In Figure 2, the warming thermogram of 33 wt %  $(\text{NH}_4)_2\text{SO}_4$  emulsion of  $\sim 58.9$  mg (marked by 33 wt % (L),

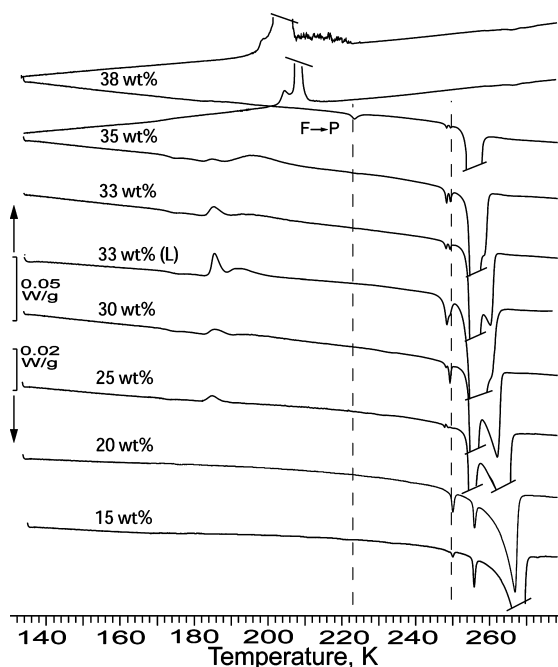


**Figure 2.** Thermograms obtained from emulsified micrometer-scaled 15–38 wt %  $(\text{NH}_4)_2\text{SO}_4$  droplets. The large truncated freezing event in the cooling thermogram (shown only for 35 and 38 wt %  $(\text{NH}_4)_2\text{SO}_4$  samples) is a result of simultaneous freezing out of pure ice and the freezing of a residual solution.<sup>28</sup> The mass of emulsion samples is  $25 \pm 3$  mg. The mass of 33 wt % (L) sample is  $\sim 58.90$  mg (see text for details). The small double endothermic peak at  $\sim 249$  K is due to the eutectic melting of ice/letovicite II and ice/letovicite III.<sup>33</sup> The other two melting events are the same as in Figure 1. In the 38 wt %  $(\text{NH}_4)_2\text{SO}_4$  warming thermogram, the two melting events overlap completely. The droplets of composition 15–25 wt %  $(\text{NH}_4)_2\text{SO}_4$  have diameter between  $\sim 1$  and  $25 \mu\text{m}$ , the droplets of 30–35 wt %  $(\text{NH}_4)_2\text{SO}_4$  between  $\sim 1$  and  $80 \mu\text{m}$ , and those of 38 wt %  $(\text{NH}_4)_2\text{SO}_4$  between  $\sim 1$  and  $120 \mu\text{m}$ . Two scale bars, which denote the heat flow through samples, correspond to the two groups of thermograms marked by arrows.

“large”) is shown as an example. It can be seen that the increased emulsion mass, and consequently the increased amount of  $\text{H}_2\text{O}$  and  $(\text{NH}_4)_2\text{SO}_4$ , results in an increased area of the corresponding three melting peaks, as expected, but does not result in the appearance of the  $\text{F} \rightarrow \text{P}$  transition. That is, option (i) is falsified.

To test the second option, we determined the “mass sensitivity” of Mettler Toledo DSC 822 to detect the ferroelectric transition. To this end, we measured several samples of finely powdered 99.99%  $(\text{NH}_4)_2\text{SO}_4$ . Optical and electron microscope measurements (not shown) reveal that  $(\text{NH}_4)_2\text{SO}_4$  crystals are mainly of  $\sim 1 \pm 0.2 \mu\text{m}$  in size although there are crystals much smaller than this size. The powdered crystals are sintered and form aggregates and agglomerates from several to tens of micrometers long. Thermograms obtained from four samples of progressively reduced mass of finely powdered  $(\text{NH}_4)_2\text{SO}_4$  are presented in Figure 3. It is seen that all thermograms contain the  $\text{P} \rightarrow \text{F}$  and  $\text{F} \rightarrow \text{P}$  transitions. The decreasing area under the transition peaks is due to the reduced mass of  $(\text{NH}_4)_2\text{SO}_4$  participating in the transitions. The  $\text{P} \rightarrow \text{F}$  and  $\text{F} \rightarrow \text{P}$  transitions are clearly seen even in the thermogram obtained from a sample of merely 12  $\mu\text{g}$ . Note this mass is  $\sim 50$  times smaller than the mass of  $(\text{NH}_4)_2\text{SO}_4$  dispersed in emulsified samples employed for

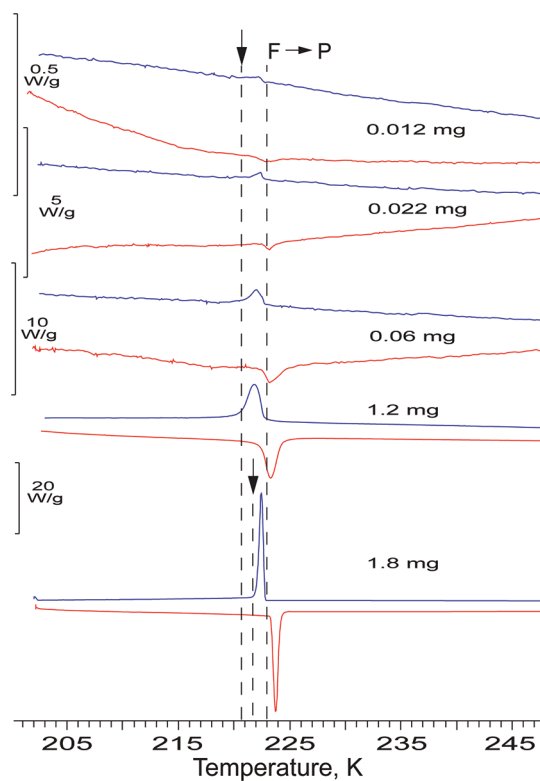


**Figure 3.** Ferroelectric transition at  $\sim 223$  K of four samples of finely powdered and coarse-grained (the lowest thermogram) 99.99%  $(\text{NH}_4)_2\text{SO}_4$  crystals. The size of finely powdered  $(\text{NH}_4)_2\text{SO}_4$  crystals is  $\sim 1 \pm 0.2 \mu\text{m}$  and coarse-grained ones  $\sim 0.4$ – $0.6$  mm. Two arrows show the temperature difference of  $\sim 1$  K between the end of the  $\text{P} \rightarrow \text{F}$  transition of coarse-grained and finely powdered  $(\text{NH}_4)_2\text{SO}_4$  (see text for details). The mass of  $(\text{NH}_4)_2\text{SO}_4$  is indicated.

obtaining the thermograms in Figure 2. For example, the mass of  $(\text{NH}_4)_2\text{SO}_4$  dispersed in 25 mg emulsion samples varies between  $\sim 0.3$  and  $\sim 0.8$  mg, depending on droplet concentration. Thus, the sensitivity of Mettler Toledo DSC 822 is more than enough to detect the enthalpy released during the  $\text{F} \rightarrow \text{P}$  transition in  $(\text{NH}_4)_2\text{SO}_4$  crystals precipitated in the emulsified  $(\text{NH}_4)_2\text{SO}_4/\text{H}_2\text{O}$  droplets of all concentrations. Thus, option (ii) is falsified, too.

To test the third option, i.e., whether the oil/surfactant matrix results in the disappearance of the  $\text{F} \rightarrow \text{P}$  transition, we dispersed finely powdered  $(\text{NH}_4)_2\text{SO}_4$  into the oil/lanolin matrix and measured the ferroelectric transition. At first we measured  $(\text{NH}_4)_2\text{SO}_4$ -in-oil/lanolin dispersion immediately after preparation, i.e., a so-called “fresh” sample. Then we measured the same sample after 5 days. The two thermograms are displayed in Figure 4. One can see that the “fresh” and 5-day-old samples produce identical thermograms. If there were some interaction at the oil/surfactant-matrix/ $(\text{NH}_4)_2\text{SO}_4$  interface, which disturbs the electrical polarization on the surface of  $(\text{NH}_4)_2\text{SO}_4$  and consequently changes transition enthalpy, then we would have seen a change in the ferroelectric transition peaks. The identity of thermograms suggests that the oil/lanolin matrix does not impact on the appearance of the ferroelectric transition. That is, option (iii) is falsified as well. Thus, the remaining (iv) option suggests that, in contrast to millimeter-scaled droplets (see Figure 1), during the freezing of emulsified 15–35 wt %  $(\text{NH}_4)_2\text{SO}_4$  droplets (see Figure 2) ammonium sulfate precipitates into the paraelectric phase

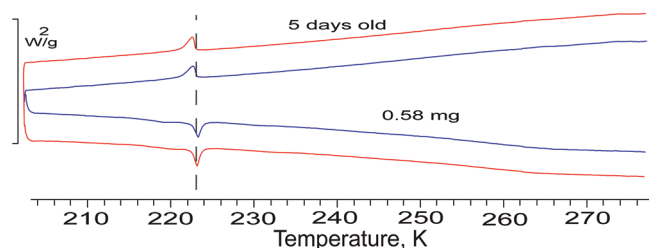


**Figure 4.** Ferroelectric transition of a “fresh” (blue lines) and the same 5-day-old (red lines) sample of finely powdered  $(\text{NH}_4)_2\text{SO}_4$  crystals dispersed in the oil/lanolin matrix. The mass of samples is indicated.

independently of whether the freezing occurs above (15 wt %  $(\text{NH}_4)_2\text{SO}_4$  droplets) or below 223 K (see Figure 10 in ref 32). In other words, similar to technologically important ferroelectrics, a critical size of  $(\text{NH}_4)_2\text{SO}_4$  exists below which the ferroelectric phase collapses. The material discussed below confirms this statement.

Figure 3 also demonstrates other finite size effects in  $(\text{NH}_4)_2\text{SO}_4$ . The lowest thermogram was obtained from coarse-grained, as supplied by the manufacturer,  $(\text{NH}_4)_2\text{SO}_4$  crystals of size of  $\sim 0.4$ – $6$  mm. It is seen that the  $\text{P} \rightarrow \text{F}$  and  $\text{F} \rightarrow \text{P}$  transition peaks are very sharp. In contrast, the transition peaks of finely powdered  $(\text{NH}_4)_2\text{SO}_4$  are diffuse (smeared) that is due to both reduced crystal sizes and their size distribution. The smeared transitions are also seen in Figure 4. In Figure 3, the shift of  $\sim 1$  K is marked by arrows which show the temperatures where the  $\text{P} \rightarrow \text{F}$  transition almost ceases. These temperatures are determined as an intersection of the low-temperature baseline and the steepest slope of the  $\text{P} \rightarrow \text{F}$  transition peak. The temperature shift is produced by the population of crystals smaller than the majority of crystals of  $\sim 1 \pm 0.2 \mu\text{m}$ .

We measured specific enthalpy,  $\Delta H_{\text{ferr}}$ , of the  $\text{P} \rightarrow \text{F}$  and  $\text{F} \rightarrow \text{P}$  transitions of several large single  $(\text{NH}_4)_2\text{SO}_4$  crystals ( $\sim 1.5$  mm) and several samples of coarse-grained  $(\text{NH}_4)_2\text{SO}_4$  crystals ( $\sim 0.4$ – $0.6$  mm) of 1.2–1.5 mg mass. We obtained the value of  $\Delta H_{\text{ferr}} \approx 11.47 \pm 1.75$  J/g. We also measured the  $\Delta H_{\text{ferr}}$  of the  $\text{P} \rightarrow \text{F}$  and  $\text{F} \rightarrow \text{P}$  transitions produced by  $(\text{NH}_4)_2\text{SO}_4$  precipitated during the freezing of millimeter-scaled droplets and obtained the value of  $\Delta H_{\text{ferr}} \approx 11.31$  J/g. These two values are similar to the literature data of  $\Delta H_{\text{ferr}} = 1.54 \pm 0.39$  kJ/mol =  $11.65 \pm 2.95$  J/g.<sup>35</sup> The similarity of the  $\Delta H_{\text{ferr}}$  of  $(\text{NH}_4)_2\text{SO}_4$  precipitated in millimeter-scaled droplets, and that of bulk  $(\text{NH}_4)_2\text{SO}_4$  crystals indicates that during the second freezing event practically all of precipitated  $(\text{NH}_4)_2\text{SO}_4$  participates in the  $\text{P} \rightarrow \text{F}$  and  $\text{F} \rightarrow \text{P}$  transitions. We write “practically” because some  $\text{NH}_4^+$  and  $\text{SO}_4^{2-}$  may be buried in ice during freezing. Using the value of  $\Delta H_{\text{ferr}} \approx 11.31$  J/g and the enthalpy of  $\sim 3.76$  mJ released during the  $\text{F} \rightarrow \text{P}$  transition in the warming 38 wt %  $(\text{NH}_4)_2\text{SO}_4$  thermogram (Figure 2), we obtained the mass of  $(\text{NH}_4)_2\text{SO}_4$  which participated in the  $\text{F} \rightarrow \text{P}$  transition. We found that only  $\sim 0.3$  mg of the total dispersed mass of  $\sim 0.8$  mg produces the  $\text{F} \rightarrow \text{P}$  transition. This means that despite the fact that 38 wt %  $(\text{NH}_4)_2\text{SO}_4$  droplets are cooled below 223 K, the majority of  $(\text{NH}_4)_2\text{SO}_4$  crystals ( $\sim 0.5$  mg) precipitate not into the ferroelectric phase but into the paraelectric phase.

The analysis of freezing thermograms in Figures 2 and 5 allows us to understand why in the 38 wt %  $(\text{NH}_4)_2\text{SO}_4$  sample only a fraction of  $(\text{NH}_4)_2\text{SO}_4$  precipitates into the paraelectric phase. The diameter of emulsified 15–38 wt %  $(\text{NH}_4)_2\text{SO}_4$

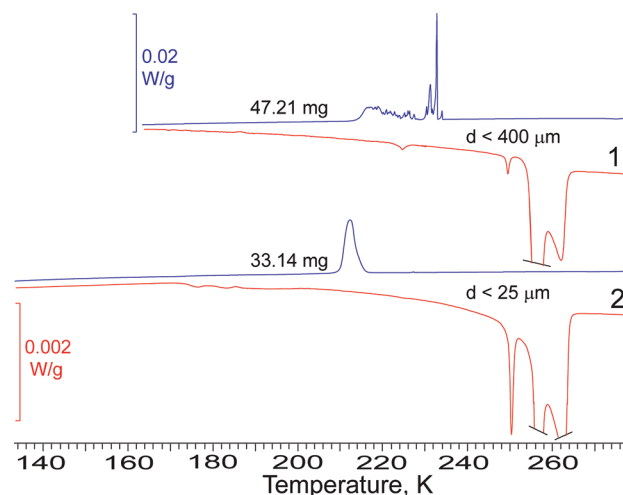


**Figure 5.** Thermograms obtained from emulsified 30 wt %  $(\text{NH}_4)_2\text{SO}_4$  droplets of two size distributions. The mass of emulsion samples and the size of the largest droplets are indicated. The blue scale bar (0.02 W/g) is only for the cooling (blue) thermograms and the red one (0.002 W/g) for the 10-fold-magnified warming (red) thermograms.

droplets employed for obtaining the thermograms in Figure 2 are given in the figure caption. Optical microscope measurements show that although 30–38 wt %  $(\text{NH}_4)_2\text{SO}_4$  emulsions contain a population of large droplets, the majority of them are in the size range of  $\sim 1$ – $25 \mu\text{m}$ . If all droplets are within a narrow size range, then they produce an approximately bell-shaped freezing peak such as in the freezing 15–30 wt %  $(\text{NH}_4)_2\text{SO}_4$  thermograms (see Figure 1b in ref 28) and in the thermogram “2” in Figure 5. If, however, a fraction of droplets is larger than the majority of the droplets, they freeze at warmer temperatures and produce a “sawlike” freezing region, such as in the topmost thermogram in Figure 2 and thermogram “1” in Figure 5. If emulsified droplets show a bimodal size distribution, then they produce two partly overlapping bell-shaped freezing peaks as is seen in the two topmost thermograms in Figure 2.

What was discussed in the previous paragraph suggests that it is the “sawlike” region in the 38 wt %  $(\text{NH}_4)_2\text{SO}_4$  thermogram (Figure 2) which is responsible for the appearance of the  $\text{F} \rightarrow \text{P}$  transition. Similar to millimeter-scaled droplets, the freezing of large emulsified droplets produces  $(\text{NH}_4)_2\text{SO}_4$  crystals large enough to form the ferroelectric phase at  $T < 223$  K. To test this statement, we measured 25–38 wt %  $(\text{NH}_4)_2\text{SO}_4$  emulsions with large size-distributed droplets. In Figure 5, thermograms obtained from 30 wt %  $(\text{NH}_4)_2\text{SO}_4$  emulsions are presented as an example. Thermogram “1” is obtained from an emulsion sample (47.21 mg) whose droplets are distributed between  $\sim 1$  and  $400 \mu\text{m}$  (see Figure 6a). The “sawlike” region and a few sharp freezing peaks indicate that in the sample there is a population of large droplets with a few very large droplets, judging from their higher freezing temperatures. In the warming thermogram “1”, the  $\text{F} \rightarrow \text{P}$  transition, which absorbs the enthalpy of  $\sim 2.7$  mJ, is clearly seen. The total mass of  $(\text{NH}_4)_2\text{SO}_4$  in the 47.21 mg sample is  $\sim 1.2$  mg. However, the mass of  $(\text{NH}_4)_2\text{SO}_4$  which produces the  $\text{F} \rightarrow \text{P}$  transition, is only  $\sim 0.2$  mg. Thermogram “2” is obtained from a sample (33.14 mg) of the same emulsion after additional stirring. This additional stirring reduces the size of the larger droplets to  $< \sim 25 \mu\text{m}$  (see Figure 6b). In the warming thermogram “2”, there is no indication of the  $\text{F} \rightarrow \text{P}$  transition. Thus, Figure 5

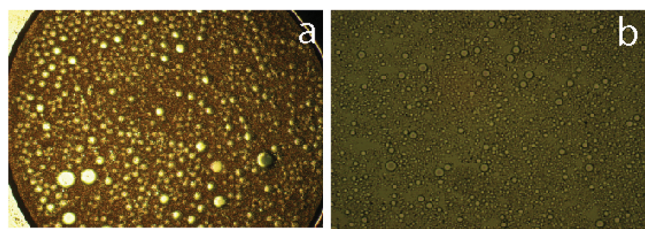


**Figure 6.** Optical microscope pictures of 30 wt %  $(\text{NH}_4)_2\text{SO}_4$  emulsions with droplets  $<sim 400 \mu\text{m}$  (a) and  $<sim 25 \mu\text{m}$  (b). The emulsion (b) was prepared by the additional stirring of the emulsion (a).

clearly demonstrates that the F  $\rightarrow$  P transition is produced by  $(\text{NH}_4)_2\text{SO}_4$  crystals precipitated from large droplets which create the “sawlike” region. While larger droplets precipitate  $(\text{NH}_4)_2\text{SO}_4$  into the ferroelectric phase, small droplets precipitate into the paraelectric phase. Only droplets larger than  $\sim 80 \mu\text{m}$  in diameter can produce ferroelectric  $(\text{NH}_4)_2\text{SO}_4$  crystals below 223 K, judging from the absence of the F  $\rightarrow$  P transition in the warming 30 wt %  $(\text{NH}_4)_2\text{SO}_4$  thermogram in Figure 2. In large droplets, which freeze at warmer temperature, precipitated  $(\text{NH}_4)_2\text{SO}_4$  crystals can be large enough to form the ferroelectric phase below 223 K. In contrast, in small droplets, the amount of  $(\text{NH}_4)_2\text{SO}_4$  is small and therefore precipitated  $(\text{NH}_4)_2\text{SO}_4$  crystals are paraelectric. The above-discussed accounts for the absence of the F  $\rightarrow$  P transition in the thermograms obtained from emulsified 0–42 wt %  $(\text{NH}_4)_2\text{SO}_4$  droplets in ref 29. In that work, the average droplet diameter ranges from 5.6 to 11  $\mu\text{m}$  with the standard deviation from 2.1 to 5.9  $\mu\text{m}$ . These sizes are similar to our droplets in which  $(\text{NH}_4)_2\text{SO}_4$  precipitates into the paraelectric phase below 223 K. The fact that, depending on droplets size, at temperature below 223 K ammonium sulfate precipitates either into the ferroelectric or paraelectric phase suggests that  $(\text{NH}_4)_2\text{SO}_4$  “feels” when there is enough material to form an ordered ferroelectric domain structure. In other words, a critical size of  $(\text{NH}_4)_2\text{SO}_4$  exists below which the ferroelectric phase cannot be formed.

Concentration and degree of supercooling of droplets can also affect the size of precipitated  $(\text{NH}_4)_2\text{SO}_4$  crystals. Millimeter-scaled droplets start freezing at relatively low supercooling. Therefore, they freeze in two steps.<sup>31</sup>  $(\text{NH}_4)_2\text{SO}_4$  crystals capable of forming the ferroelectric phase precipitate during the freezing of the residual solution whose concentration is eutectic ( $\sim 40$  wt %  $(\text{NH}_4)_2\text{SO}_4$ )<sup>31</sup> or larger.<sup>32</sup> Large emulsified droplets, which form the “sawlike” region in Figures 2 and 5, may also freeze in two steps and produce ferroelectric  $(\text{NH}_4)_2\text{SO}_4$  crystals below 223 K. In contrast, the supercooling of small-sized droplets reaches up to  $\sim 20$  K which is larger than that of millimeter-scaled and large emulsified droplets. The freezing out of pure ice in small-sized droplets starts within or below “the  $\sim 210$ – $225$  K region”.<sup>28</sup> Since the residual solution tends to freeze in the  $\sim 210$ – $225$  K region,<sup>28</sup> the small-sized droplets freeze practically in one step. Because of the fact that this one-step freezing process occurs much below the eutectic temperature,  $\sim 254.5$  K,<sup>31</sup> it produces a solid mixture of very small ice and  $(\text{NH}_4)_2\text{SO}_4$  crystallites. The  $(\text{NH}_4)_2\text{SO}_4$  crystallites can be smaller than the critical size of  $(\text{NH}_4)_2\text{SO}_4$ . Thus, the size, concentration, and supercooling of  $(\text{NH}_4)_2\text{SO}_4/\text{H}_2\text{O}$  droplets govern the size of precipitated  $(\text{NH}_4)_2\text{SO}_4$  crystals and consequently the formation of ferro- or paraelectric phase.

While our microscopic approach allows for the measurement of droplet size, we cannot directly measure the size of  $(\text{NH}_4)_2\text{SO}_4$  crystals precipitated during the freezing of emulsified droplets. However, we can qualitatively estimate an upper limit for the critical size of  $(\text{NH}_4)_2\text{SO}_4$ . In Figure 3, the fact that the ferroelectric transition is only slightly ( $\sim 1$  K) shifted to temperature colder than  $T_c \approx 223$  K indicates that the critical size may be much smaller than  $1 \pm 0.2 \mu\text{m}$ . Further, Fourier transform infrared (FTIR) measurements detected changes in the indices of refraction for  $(\text{NH}_4)_2\text{SO}_4$  particles of size between  $\sim 0.1$  and  $1 \mu\text{m}$  at  $T < 223$  K.<sup>36</sup> The changes in the indices of refraction were assumed to be brought about by the ferroelectric transition. If so, then the critical size of  $(\text{NH}_4)_2\text{SO}_4$  should be smaller than 100 nm. Comparing the molecular structure and the number of atoms in unit cell of  $(\text{NH}_4)_2\text{SO}_4$  with that of  $\text{SrBi}_2\text{Ta}_2\text{O}_9$  and  $\text{PbTiO}_3$ , of which critical sizes were determined to be  $\sim 2.6$  nm<sup>1</sup> and  $8.2$  nm,<sup>2</sup> respectively, one may assume that the critical size of  $(\text{NH}_4)_2\text{SO}_4$  may be even less than 10 nm.

## CONCLUSIONS

We have presented calorimetric results which demonstrate that similar to other ferroelectrics, for example,  $\text{SrBi}_2\text{Ta}_2\text{O}_9$ ,<sup>1</sup>  $\text{PbTiO}_3$ ,<sup>2,7</sup> and  $\text{BaTiO}_3$ ,<sup>9</sup> the finite size effects such as the smeared ferroelectric transition, the shift of the Curie temperature of  $T_c \approx 223$  K to lower temperature, and critical size exist also in  $(\text{NH}_4)_2\text{SO}_4$ . In particular, we show that finely powdered  $(\text{NH}_4)_2\text{SO}_4$  crystals of size  $1 \pm 0.2 \mu\text{m}$  produce the ferroelectric transition which is smeared in comparison with the sharp transition of coarse-grained crystals of size  $\sim 0.4$ – $0.6 \mu\text{m}$ . The shift of  $\sim 1$  K to colder temperature of the ferroelectric transition is accounted for by the presence of a population of  $(\text{NH}_4)_2\text{SO}_4$  crystals smaller than  $1 \pm 0.2 \mu\text{m}$ . We also show that (emulsified) large micrometer-sized droplets precipitate  $(\text{NH}_4)_2\text{SO}_4$  into the ferroelectric phase during freezing below 223 K, whereas small ( $<sim 25 \mu\text{m}$ ) droplets precipitate into the paraelectric phase. The fact that below 223 K ammonium sulfate precipitates either into the ferroelectric or paraelectric phase suggests that a critical size of  $(\text{NH}_4)_2\text{SO}_4$  exists below which the ferroelectric phase cannot be formed. Although our results do not allow us to estimate the exact critical size of  $(\text{NH}_4)_2\text{SO}_4$ , from independent measurements on  $(\text{NH}_4)_2\text{SO}_4$  aerosol particles,<sup>36</sup> we conclude it to be less than 100 nm. Further measurements, using other experimental techniques, are needed in order to determine the precise value of the critical size of  $(\text{NH}_4)_2\text{SO}_4$ .

## AUTHOR INFORMATION

### Notes

The authors declare no competing financial interest.

## ACKNOWLEDGMENTS

The authors are thankful for financial support by the Austrian Science Fund (project P23027) and by the ERC (Starting Grant SULIWA). A.B. thanks the Chemical and Physical departments of the University of Helsinki for providing facilities for the performance of experiments.

## REFERENCES

- Yu, T.; Shen, Z. X.; Toh, W. S.; Xue, J. M.; Wang, J. *J. Appl. Phys.* **2003**, *94*, 618–620.
- Ishikawa, K.; Nagareda, K. *J. Korean Phys. Soc.* **1998**, *32*, S56–S58.

- (3) Fong, D. D.; Stephenson, G. B.; Streiffer, S. K.; Eastman, J. A.; Auciello, O.; Fuoss, P. H.; Thompson, C. *Science* **2004**, *304*, 1650–1653.
- (4) Shaoping, L.; Eastman, J. A.; Li, Z.; Foster, C. M.; Newnham, R. E.; Cross, L. E. *Phys. Lett. A* **1996**, *212*, 341–346.
- (5) Spanier, J. E.; Kolpak, A. M.; Urban, J. J.; Grinberg, I.; Ouyang, L.; Yun, W. S.; Rappe, A. M.; Park, H. *Nano Lett.* **2006**, *6*, 735–739.
- (6) Chattopadhyay, S. *Nanostruct. Mater.* **1997**, *9*, 551–554.
- (7) Despont, L.; Koitzsch, C.; Clerc, F.; Garnier, M. G.; Aebi, P.; Lichtensteiger, C.; Triscone, J.-M.; Garcia de Abajo, F. J.; Bousquet, E.; Ghosez, Ph. *Phys. Rev. B* **2006**, *73*, 094110.
- (8) Junquera, J.; Ghosez, P. *Nature* **2003**, *422*, 506–509.
- (9) Garcia, V.; Fusil, S.; Bouzehouane, K.; Enouz-Vedrenne, S.; Mathur, N. D.; Barthelemy, A.; Bibes, M. *Nature* **2009**, *460*, 81–84.
- (10) Meneses, D. de S.; Hauret, G.; Simon, P. *Phys. Rev. B* **1995**, *51*, 2669–2677.
- (11) Guimaraes, F. E. G.; Chaves, A. S.; Ribeiro, G. M.; Gazzinelli, R. *J. Phys.: Condens. Matter* **1992**, *4*, 6467–6472.
- (12) Schutte, C. J. H.; Heyns, A. M. *J. Chem. Phys.* **1970**, *52*, 864–871.
- (13) Misra, S. K.; Sun, J.; Jerzak, S. *Phys. Rev. B* **1989**, *40*, 74–83.
- (14) Gridnev, S. A.; Safonova, L. P.; Ivanov, O. N.; Davydova, T. V. *Phys. Solid State* **1998**, *40*, 1998–2001.
- (15) Bhat, H. L.; Clark, G. F.; Klapper, H.; Roberts, K. J. *J. Phys. D: Appl. Phys.* **1995**, *28*, A23–A26.
- (16) Jain, Y. S.; Bist, H. D. *Phys. Status Solidi* **1974**, *62*, 295–300.
- (17) O'Railly, D. E.; Tsang, T. *J. Chem. Phys.* **1967**, *46*, 1291–1300.
- (18) Sawada, A.; Takagi, Y.; Ishibashi, Y. *J. Phys. Soc. Jpn.* **1973**, *34*, 748–754.
- (19) Badr, Y. A.; Awad, S. *Phys. Status Solidi A* **1982**, *72*, K27–K31.
- (20) Tsou, N. T.; Potnis, P. R.; Huber, J. E. *Phys. Rev. B* **2011**, *83*, 184120.
- (21) Abbatt, J. P. D.; Benz, S.; Czicz, D. J.; Kanji, Z.; Lohman, U.; Mohler, O. *Science* **2006**, *313*, 1770–1773.
- (22) Pruppacher, H. R.; Klett, J. D. *Microphysics of Clouds and Precipitation*; Kluwer: Dordrecht, 1997.
- (23) Li, D.; Zhao, M. H.; Garra, J.; Kolpak, A. M.; Rappe, A. M.; Bonnell, D. A.; Vohs, J. M. *Nat. Mater.* **2008**, *7*, 473–477.
- (24) Yun, Y.; Altman, E. I. *J. Am. Chem. Soc.* **2007**, *129*, 15684–15689.
- (25) Levchenko, S. V.; Rappe, A. M. *Phys. Rev. Lett.* **2008**, *100*, 256101.
- (26) Kolpak, A. M.; Grinberg, I.; Rappe, A. M. *Phys. Rev. Lett.* **2007**, *98*, 166101.
- (27) Pruppacher, H. R. *Pure Appl. Geophys.* **1973**, *104*, 623–634.
- (28) Bogdan, A.; Molina, M. J.; Tenhu, H.; Mayer, E.; Bertel, E.; Loerting, T. *J. Phys.: Condens. Matter* **2011**, *23*, 035103 (6pp).
- (29) Bertram, A. K.; Koop, T.; Molina, L. T.; Molina, M. J. *J. Phys. Chem. A* **2000**, *104*, 584–588.
- (30) Chang, H.-Y. A.; Koop, T.; Molina, L. T.; Molina, M. J. *J. Phys. Chem.* **1999**, *103*, 2673–2679.
- (31) Bogdan, A. *J. Phys. Chem. A* **2010**, *114*, 10135–10139.
- (32) Bogdan, A.; Loerting, T. *J. Phys. Chem. C* **2011**, *115*, 10682–10693.
- (33) Bogdan, A.; Molina, M. J.; Tenhu, H.; Loerting, T. *Phys. Chem. Chem. Phys.* **2011**, *13*, 19704–19706.
- (34) Höhne, G.; Hemminger, W.; Flammershain, H.-J. *Differential Scanning Calorimetry*; Springer: Berlin, 1995.
- (35) Beyer, K. D.; Bothe, J. R.; Burrmann, N. *J. Phys. Chem. A* **2007**, *111*, 479–494.
- (36) Earle, M. E.; Pancescu, R. G.; Cosic, B.; Zsetsky, A. Y.; Sloan, J. *J. Phys. Chem. A* **2006**, *110*, 13022–13028.